LA-2142
C.3

LOS ALAMOS SCIENTIFIC LABORATORY
OF THE UNIVERSITY OF CALIFORNIA ○ LOS ALAMOS   NEW MEXICO

PRELIMINARY CRITICAL EXPERIMENTS ON A MOCK-UP
OF THE LOS ALAMOS MOLTEN PLUTONIUM REACTOR

LEGAL NOTICE

LA-2142
REACTORS - POWER
(TID-4500, 13th ed., suppl.)

LOS ALAMOS SCIENTIFIC LABORATORY
OF THE UNIVERSITY OF CALIFORNIA   LOS ALAMOS   NEW MEXICO

REPORT WRITTEN: June 1957

REPORT DISTRIBUTED: April 15, 1958

PRELIMINARY CRITICAL EXPERIMENTS ON A MOCK-UP
OF THE LOS ALAMOS MOLTEN PLUTONIUM REACTOR

Work done by:

H. G. Barkmann
B. M. Carmichael
D. M. Holm
R. M. Kiehn
R. E. Peterson
D. E. Schwarzer
J. W. Woolsey
J. Grundl
R. G. Wagner
T. F. Wimett
R. H. White

Report written by:

H. G. Barkmann
D. M. Holm
R. M. Kiehn
R. E. Peterson

1

ABSTRACT

A series of measurements of critical masses has been made for
fast-spectrum plutonium assemblies similar to proposed designs for
the Los Alamos Molten Plutonium Reactor Experiment (LAMPRE I). The
effectiveness of various systems of reactivity control has been
determined. Fission rate distributions and spatial flux variations
were obtained for comparison with values computed according to the
S_n method.

INTRODUCTION

The purpose of the series of measurements was to obtain experience with small, complex plutonium assemblies that have a very fast neutron spectrum and metal reflectors. Points of specific interest in the measurements were:

1. The establishment of the critical mass of an assembly which approximated a possible design for a 1 Mw molten plutonium reactor with metal cooling (LAMPRE I).

2. The effectiveness of various control schemes based on reflector replacement.

3. The determination of power and flux distributions in the reactor mock-up as a guide to making proper choices of reflector thicknesses in a finished reactor design.

1. MECHANICAL ARRANGEMENT OF THE CRITICAL EXPERIMENT

The critical experiments were done using a basic assembly machine at the LASL critical assembly facility located at Pajarito Site. The mock-up of the reactor core was assembled by hand; the mechanical insertion of the very subcritical bare core into the reflector portion of the reactor mock-up was then accomplished by remote control. Two independent fail-safe (gravity operated) scrams were provided to comply with safety requirements for delayed critical operation: retraction of the core from reflector and dropping of the control shim.

Figure 1.1 shows the mechanical arrangement of the LAMPRE critical experiment (L.C.X.). The water tank simulates the water shield proposed for the reactor. The radial and top portions of the metal (Fe or Ni) neutron reflector are shown in place inside the central tube of the water tank. This central tube isolates the fissionable material of the core from the water. The lower half of the assembly, which carries the cylindrical "cage" containing the core components, was raised by remotely controlled operation of a hydraulic lift. The "core cage" rests

VACUUM LATCH
FOR SHIM SCRAM

ANNULAR WATER
DISPLACEMENT
CONTROL SHIM

CONTROL
SHIM MOTION

WATER CONTAINER

B^{10} COUNTER

TOP REFLECTOR
PLUG

RADIAL
REFLECTOR
SLEEVE

Ta CORE SLEEVE

LOWER REFLECTOR
PLUG

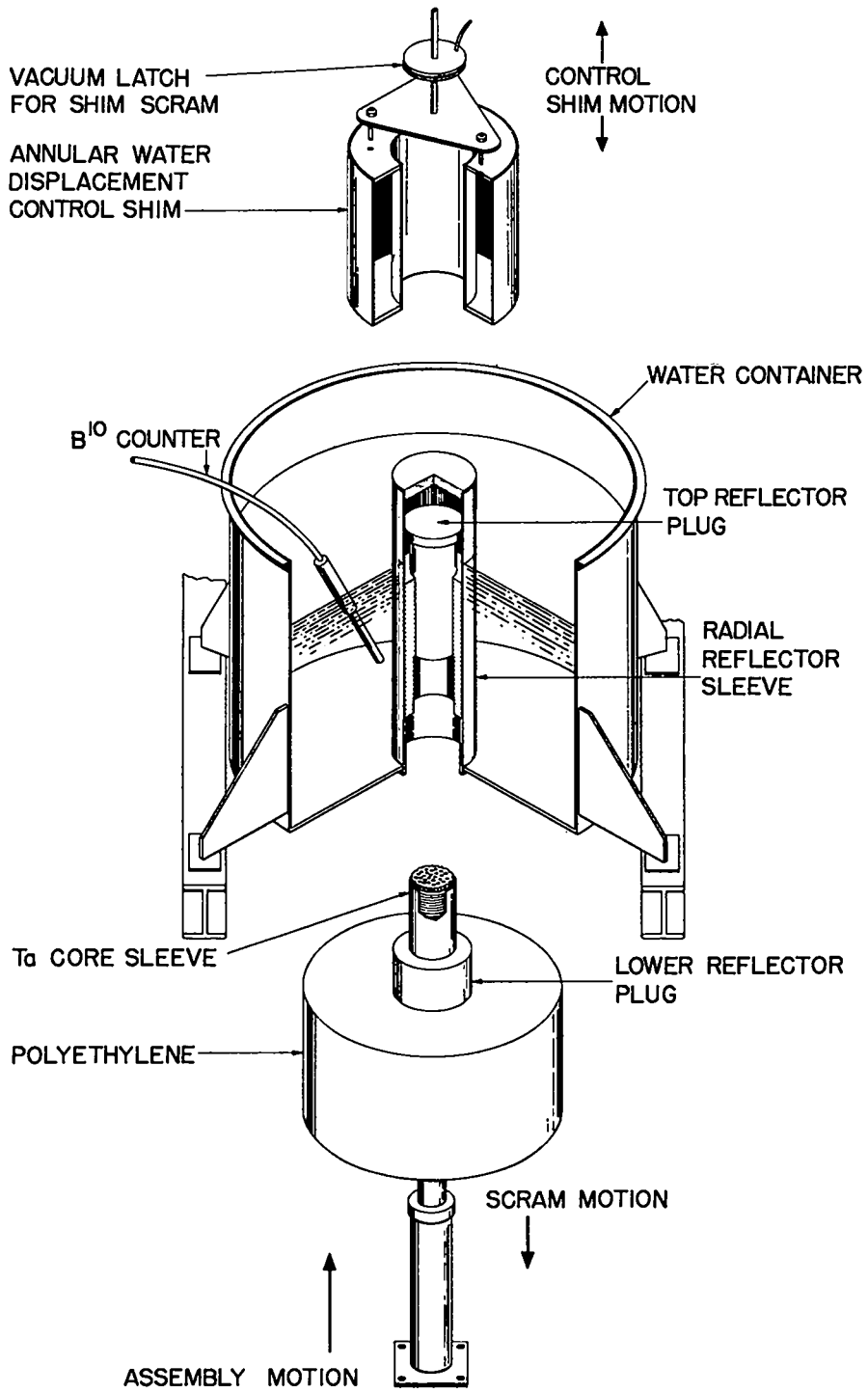POLYETHYLENE

SCRAM MOTION

ASSEMBLY MOTION

Fig. 1.1 Cutaway view of LAMPRE critical experiment.

6

on the bottom section of the metal reflector, which is in turn supported
by a large polyethylene block. For convenience, polyethylene was used
in place of water as a shield mock-up in this portion of the assembly.

Figure 1.2 is a cross section view of the assembled critical
experiment which indicates the relative positions of the radial reflec-
tor, the top and bottom reflectors, and a typical control shim which
displaces water from the vicinity of the core. The radial reflector
was supported on a ledge inside the bottom of the central tube of the
water tank. The top reflector was a sliding fit in the radial reflector
and was prevented from dropping through the radial reflector by mechani-
cal stops. The lower end of the top reflector was allowed to enter the
core cage and rest on the core components, thus ensuring that the core
components were held under a constant compressive load of about 60 lb.
Immediately above and below the core 0.7 in. thick aluminum discs, re-
duced to an average density of about 33% of normal by appropriate hole
drilling, were used to simulate sodium-filled coolant plenums. A sim-
ilar plenum was located below the bottom metal reflector.

The control shim (shown in Fig. 1.2) was solid aluminum; a similar
hollow annular shim fabricated from 1/32 in. stainless steel was also
provided. For additional tests of control system effectiveness the
hollow shim could be filled with B_4C (see Section 2).

The effect of changing the thickness of the radial tamper from a
nominal 1-5/8 in. to 2-3/8 in. could be studied by placing an additional
iron or nickel sleeve outside the central tube of the water tank
(Section 2). Control shims with correspondingly larger inner and outer
diameters were provided for these cases.

The proposed core for LAMPRE I was to be composed of 76% (by
volume) of fuel (Pu-Ni alloy), 17% coolant (Na), and 7% core container
and coolant flow tubes (Ta). In the L.C.X. the sodium was represented
by low-density aluminum, the replacement being made on an approximately
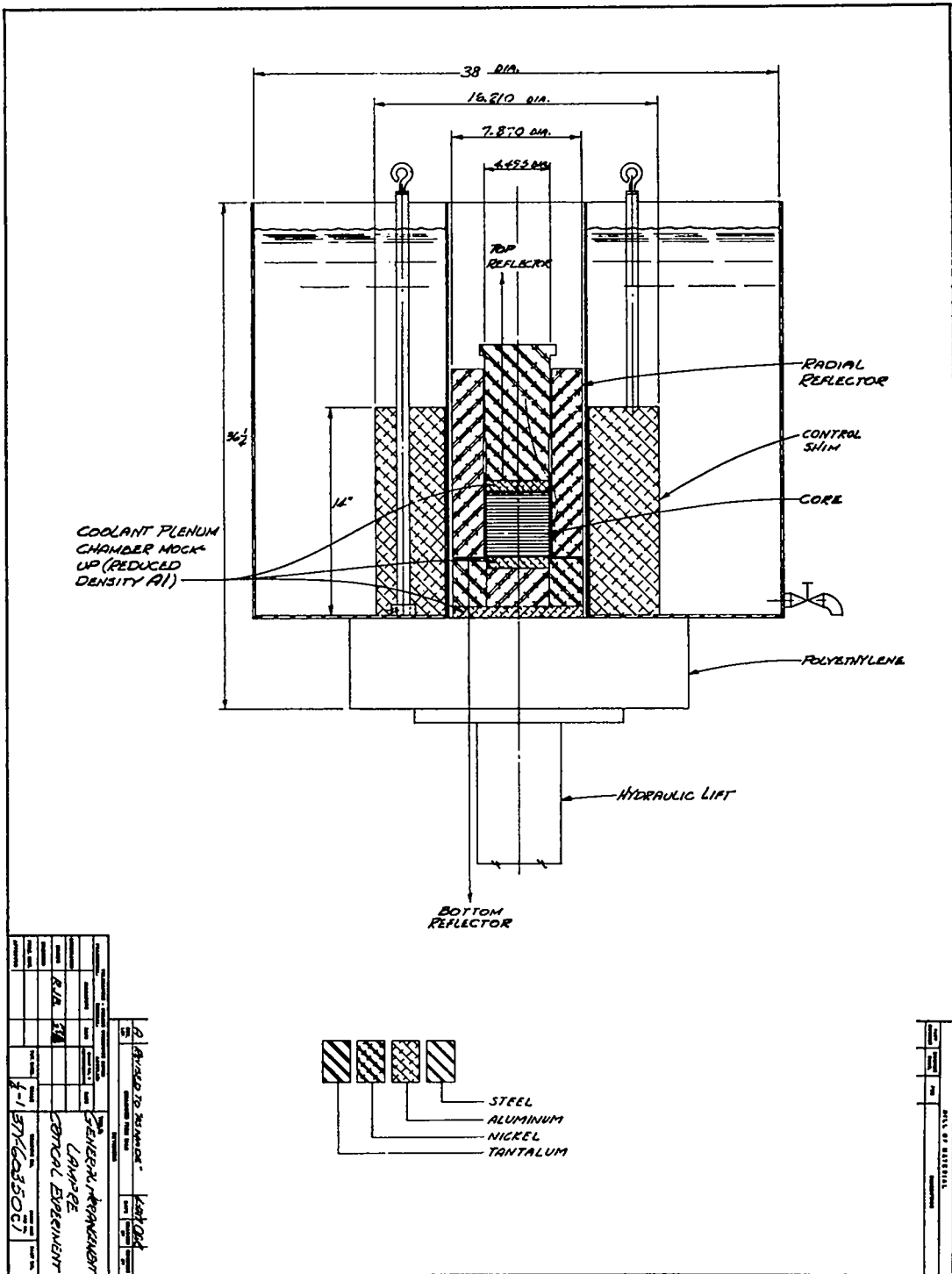atom for atom basis. The fuel alloy was simulated by nickel-coated

Fig. 1.2 Cross section view of LAMPRE critical experiment.

8

plutonium. Core materials were introduced into the L.C.X. in the form of discs of appropriate thicknesses to yield the specified relative volumes of each component.

Figure 1.3 is a photograph of the core cage, the lower reflector section, and discs of core component materials. The nickel-coated plutonium discs were 4.499 in. in diameter and 0.136 in. thick, including about 0.006 in. of nickel coating on all surfaces. Tantalum discs were 4.500 in. in diameter and 0.014 in. thick; the aluminum discs were of the same diameter but 0.027 in. thick. Pie-shaped pieces of fuel ($45°$ and $22-1/2°$ sectors of a full disc) were available for making small mass adjustments during fuel loading (Fig. 1.3). The density of a typical nickel-coated fuel plate was about 15.1 g/cm^3.

The core cage (Fig. 1.3) was built up from a tantalum cylinder (4.52 in. i.d. by 0.050 in. wall) inside an aluminum cylinder with 0.80 in. thick walls. The tantalum represented the shell of the reactor core and heat exchanger assembly, while the aluminum simulated sodium coolant in an annular space between core and reflector. Tantalum discs 0.050 in. thick were placed at the top and bottom of the stack of core component discs to mock up the tube sheets of the tube and shell heat exchanger which forms the LAMPRE core.

Figure 1.4 is an over-all view of the assembly machine. The hydraulic lift carrying the core is shown retracted to the position used for manual loading of the discs into the core cage. The hydraulic cylinder at the top of the machine was used to adjust the position of the control shim.

Sufficient numbers of neutrons for multiplication measurements were provided by the spontaneous fissions in the fuel plates; therefore, no mechanism was required for inserting a neutron source into the core.
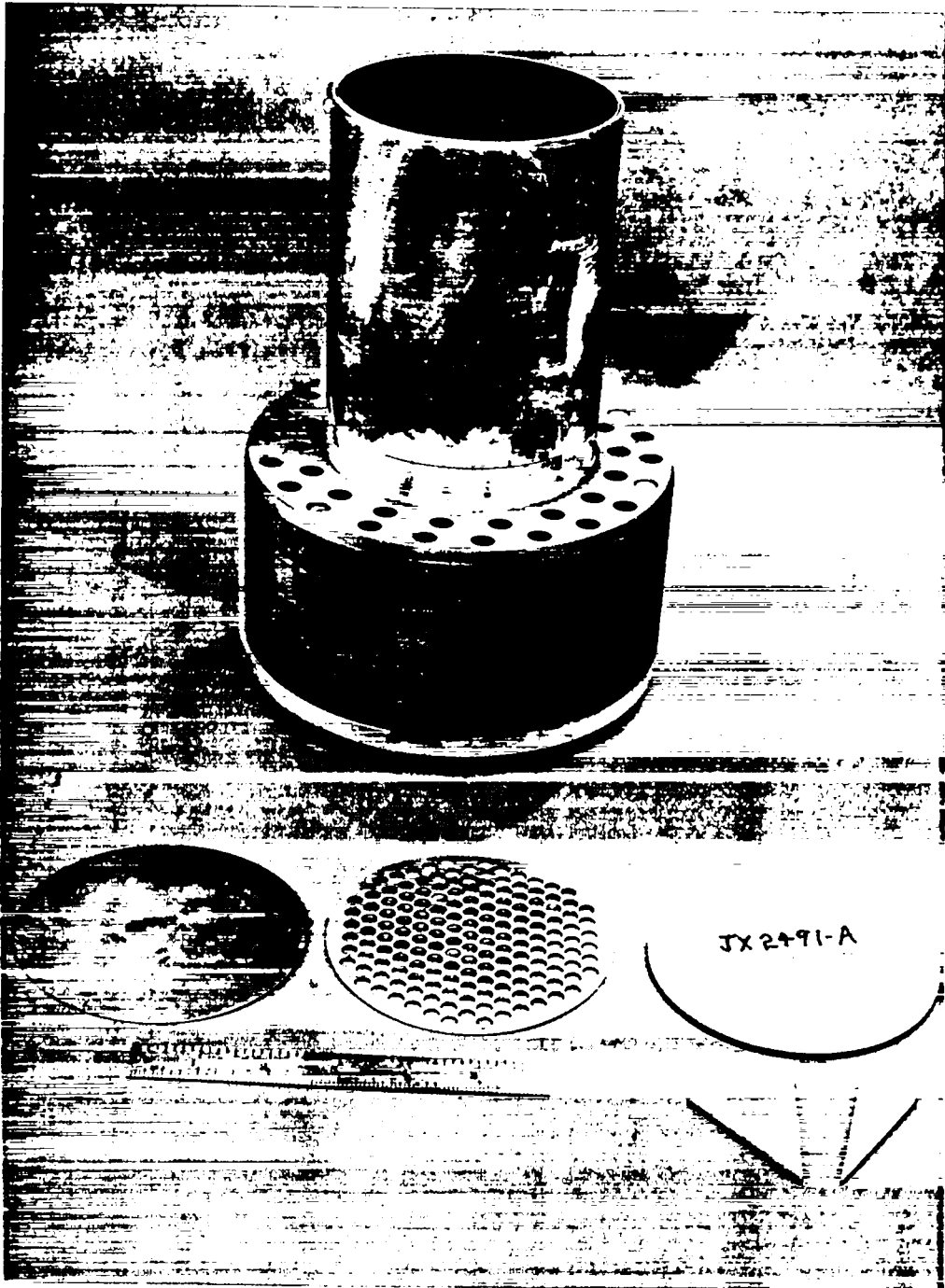
Fig. 1.3 L.C.X. core, showing core cage, lower reflector, tantalum
disc, reduced density aluminum disc, plutonium fuel disc,
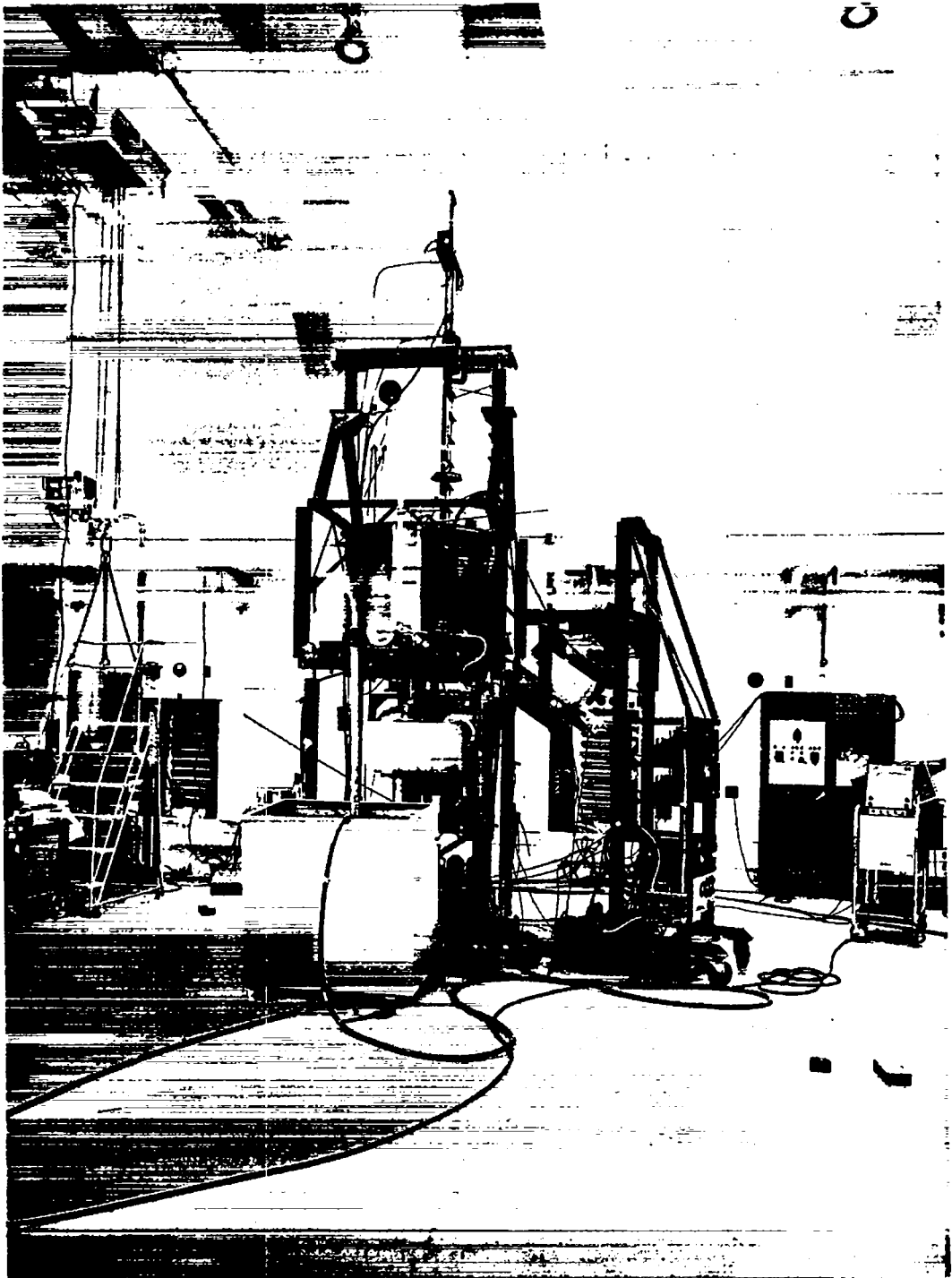and fuel disc sectors.

Fig. 1.4 L.C.X. assembly machine.

2. CRITICAL MASSES AND CONTROL SHIM EFFECTIVENESS

This portion of the experimental work was divided into two sections:

a. The determination of critical masses for several reflector and
    core composites.

b. The measurement of the effectiveness of various schemes of re-
    activity control, the evaluation of this effectiveness in terms
    of an equivalent surface mass of fuel added to the core, and
    the interpretation of surface mass in terms of reactivity
    (cents).

2.1 Critical Mass Determinations

The critical mass measurements were made with combinations of
three core and three reflector compositions. Table 2.1 lists the re-
flector arrangements; the thickness of each of the components enclosing
the core in the radial and axial directions is indicated. All cores
were based on a plutonium-nickel fuel consisting of plutonium coated
with nickel. In all cases the diameter of the cylindrical core was
fixed (nominal diameter 4.5 in.), and the system was brought to criti-
cal by adjustment of the core height. The basic building block used
in forming a core could thus be (1) a plutonium disc, (2) a plutonium
disc plus a tantalum disc, or (3) one each of the plutonium, tantalum,
and aluminum discs, depending on the core composition being studied.

The results of the basic critical mass determinations are listed
in Table 2.2. The various reflectors may be identified by reference
to Table 2.1. The designations of the core structure (Pu, Ta, Al, or
Pu, Ta, etc.) indicate which of the diluent material discs were com-
bined with each fuel disc. Nominal values for the atom densities of
the core components are also given for each core in Table 2.2. Atom
densities listed were computed on the basis of average fuel plate and
diluent plate masses and dimensions. They are representative of the
composition of the main portion of the core but not of the end region
of the core where less than a full fuel plate may have been added.

TABLE 2.1 REFLECTOR COMBINATIONS USED IN L.C.X. AND POSITION OF COMPONENTS RELATIVE TO THE CENTER OF THE CORE

Reflector	Radial Traverse			Axial Traverse (Down)			Axial Traverse (Up)		
	Inner Radius (in.)	Outer Radius (in.)	Material	Top Level (in.)	Bottom Level (in.)	Material	Bottom Level (in.)	Top Level (in.)	Material
Solid Ni	0	2.26	Core	0	$h/2$[a]	Core	0	$h/2$	Core
	2.26	2.31	Ta	$h/2$	$0.08 + h/2$	Ta	$h/2$	$0.08 + h/2$	Ta
	2.31	2.39	Al	$0.08 + h/2$	$0.77 + h/2$	Al[b]	$0.08 + h/2$	$0.77 + h/2$	Al[b]
	2.39	2.44	Air	$0.77 + h/2$	$3.77 + h/2$	Ni[c]	$0.77 + h/2$	$8.77 + h/2$	Ni[c]
	2.44	3.94	Ni[c]	$3.77 + h/2$	$4.55 + h/2$	Al[b]			
	3.94	3.96	Air	$4.55 + h/2$	$16.55 + h/2$	Polyethylene			
	3.96	4.08	Fe						
	4.08	19.0	H_2O[d]						
Solid Fe	Same as for Ni reflector, but substitute "Fe" for "Ni"								
Solid Ni + Fe	0	2.26	Core	Same as for Ni reflector			Same as for Ni reflector		
	2.26	2.31	Ta						
	2.31	2.39	Al						
	2.39	2.44	Air						
	2.44	3.94	Ni						
	3.94	3.96	Air						
	3.96	4.08	Fe						
	4.08	4.86	Fe						
	4.86	19.0	H_2O						

a. h is the core height.

b. Aluminum components were used to mock up sodium coolant plenums. The aluminum components were reduced in average density to 0.33 of full density by drilling holes.

c. Nominal nickel density is 8.66 g/cm^3. The corresponding iron reflector components had a density of 7.85 g/cm^3.

d. The inner 4 in. of the water could be displaced by a 4 in. thick annular control shim. The water extended about 10 in. above the level of the typical core, while water plus 12 in. of polyethylene extended below the bottom core level for a distance of about 15 in.

13

TABLE 2.2 BASIC CRITICAL MASSES FOR VARIOUS REFLECTOR

AND CORE COMBINATIONS IN L.C.X.

Case	Reflector	Core	Critical Mass[a] (kg)	Atoms/cm^3 x 10^{-24} in Core			
				Pu	Ni	Al	Ta
I	Solid Ni	Pu, Ta, Al	15.12 - 15.15	0.0276	0.00653	0.00440	0.00385
II	Solid Ni + Fe	Pu, Ta, Al	14.55 - 14.65	0.0276	0.00653	0.00440	0.00385
III	Solid Ni + Fe	Pu, Ta	11.45	0.0328	0.00776	--	0.00458
IV	Solid Ni	Pu, Ta	11.87	0.0329	0.00777	--	0.00458
V	Solid Ni	Pu	10.86	0.0358	0.00846	--	--
VI	Solid Fe	Pu, Ta	12.84	0.0328	0.00776	--	0.00458
VII	Solid Fe	Pu, Ta, Al	16.96	0.0276	0.00653	0.00440	0.00385

a. The critical mass (M_c) tabulated is the mass of plutonium. The mass of the nickel coating on the fuel plates is not included in these figures.

The end region contained a nominal 3% of the core mass.

The experimental results given in Table 2.2 serve as normalizations which can be used to test the validity of critical mass calculations on LAMPRE-like reactor cores (see Section 4). The critical mass varies approximately as $(1/\rho)^{1.5}$, where ρ is the density of fissionable material.

2.2 Reactivity Control Tests

The basic scheme for varying the reactivity of the L.C.X. assembly was to displace the water which surrounded the cylindrical surface of the metal reflector. This displacement was effected by lowering an air-filled annular can (control shim) into the water around the metal reflector (Fig. 1.2). The void so formed in the water increased neutron leakage, thus reducing the effective multiplication of the assembly. Preliminary calculations indicated that displacing an annular volume of water about 4 in. thick would yield satisfactory control. It was also apparent that the displacement of water by some solid material might be of practical value in an actual reactor installation since there would be no problem of possible water leakage. Aluminum and B_4C were chosen for such tests to compare the relative effectiveness of reflection and absorption control.

To evaluate the worth of the control shims, a determination of the critical mass was made with the shim in place in the water. This measurement was then compared with the critical mass measurement obtained when the shim was retracted and the water allowed to surround the nickel or iron reflector. The results of the measurements are given in Table 2.3, where the value of the control shim is expressed in terms of top surface fuel mass increments. The tabulated values of M_c are for clean cores with the control shim retracted. The sum of $M_c + \Delta M_c$ is the critical mass observed with the shim inserted to displace shield water from the vicinity of the core.

Table 2.3 indicates (Cases III and IV) that removing the innermost 4 in. of water is about 0.7 as effective as removing the water

Case	Reflector	Core	Control Shim	M_c^a (kg)	ΔM_c with Shim in Place[b] (kg)	ΔM_c (%)
I	Solid Ni + Fe	Pu, Ta	4 in. air, 360°	11.45	+0.25	+2.2
II	Solid Ni	Pu, Ta	4 in. air, 360°	11.87	+0.40	+3.4
III	Solid Ni	Pu	4 in. air, 360°	10.86	+0.38	+3.5
IV	Solid Ni, no H_2O	Pu	--	11.40	+0.54	+4.7[c]
V	Solid Fe	Pu, Ta	4 in. air, 360°	12.84	+0.71	+5.5
VI	Solid Fe	Pu, Ta	4 in. air, 60°	12.84	+0.12	+0.93[d]
VII	Solid Fe, top reflector displaced	Pu, Ta	4 in. air, 60°	13.16	+0.09	+0.68[e]
VIII	Solid Fe	Pu, Ta	4 in. B_4C, 360°	12.84	-0.60	-4.7[f]
IX	Solid Fe	Pu, Ta	4 in. Al, 360°	12.84	-0.83	-6.5[g]
X	Solid Fe	Pu, Ta	3 in. Al, 360°	12.84	-0.17	-1.3[h]
XI	Solid Fe	Pu, Ta, Al	4 in. air, 60°	16.96	+0.20	+1.2

a. The critical mass (M_c) is the mass of plutonium. Nickel coating is not included in this value.

b. A positive value of ΔM_c indicates that insertion of the control shim increases the core mass required to produce a critical configuration.

c. Contribution of H_2O outside metal reflector (Case III vs IV) is equivalent to 0.54 kg of plutonium alloy.

d. Contribution of 60° annular shim is equivalent to 1/6 of 360° annular shim (Case V vs VI).

e. A 4.5 in. diameter section of top reflector was displaced upward 5.5 in. from top of core. Effect was equivalent to 0.3 kg of plutonium alloy (Case VII vs VI).

f. Note that M_c decreases by 0.6 kg when B_4C shim is inserted.

g. M_c decreases when aluminum shim is inserted.

h. The 4 in. aluminum shim was reduced in thickness to 3 in. by increasing its inner diameter. Comparison with Case IX indicates the reduction in effectiveness of the aluminum shim.

completely. Cases V and VI of Table 2.3 show that the use of a modified control shim made as a sector of the full annular shim gives control proportional to its angular size, at least for relatively large sectors. Such a shim might be utilized for a fine control of reactivity.

Case VII indicates that a longitudinal displacement of the top reflector plug does not introduce a large negative reactivity and is, therefore, not suitable as a practical control scheme for a LAMPRE device.

The effect of the aluminum control shim (Case IX) indicates that a rather large positive change in reactivity may be obtained in contrast to the negative effect associated with the air-filled or void-type shim. The use of a solid control shim in a power reactor introduces problems of cooling the shim to remove energy deposited by gamma-rays and neutrons. However, the use of a material such as aluminum, which has a high thermal conductivity and a low gamma-ray absorption coefficient, would be feasible with only moderate surface cooling.

The results of Case X indicate that the innermost 1 in. of the 4 in. aluminum shim produces 80% of the total shim effect. Thus two concentric shims could be devised to provide coarse and fine reactivity control for the aluminum-water shim system.

For the case of a plutonium-tantalum core, the control effectiveness of the air-filled shim was measured as a function of shim position. The familiar S-shaped curve obtained is shown in Fig. 2.1. The effect of the shim is negligible when raised more than 2 in. above the top of the core.

To relate the control effectiveness measured in terms of equivalent surface core mass to reactivity, several positive and negative period measurements were made. Using these measurements in conjunction with the inhour equation and the delayed neutron data of Keepin,[1] it was found that for a plutonium-tantalum core system one dollar of reactivity was equivalent to a surface core mass addition of 0.8% of the
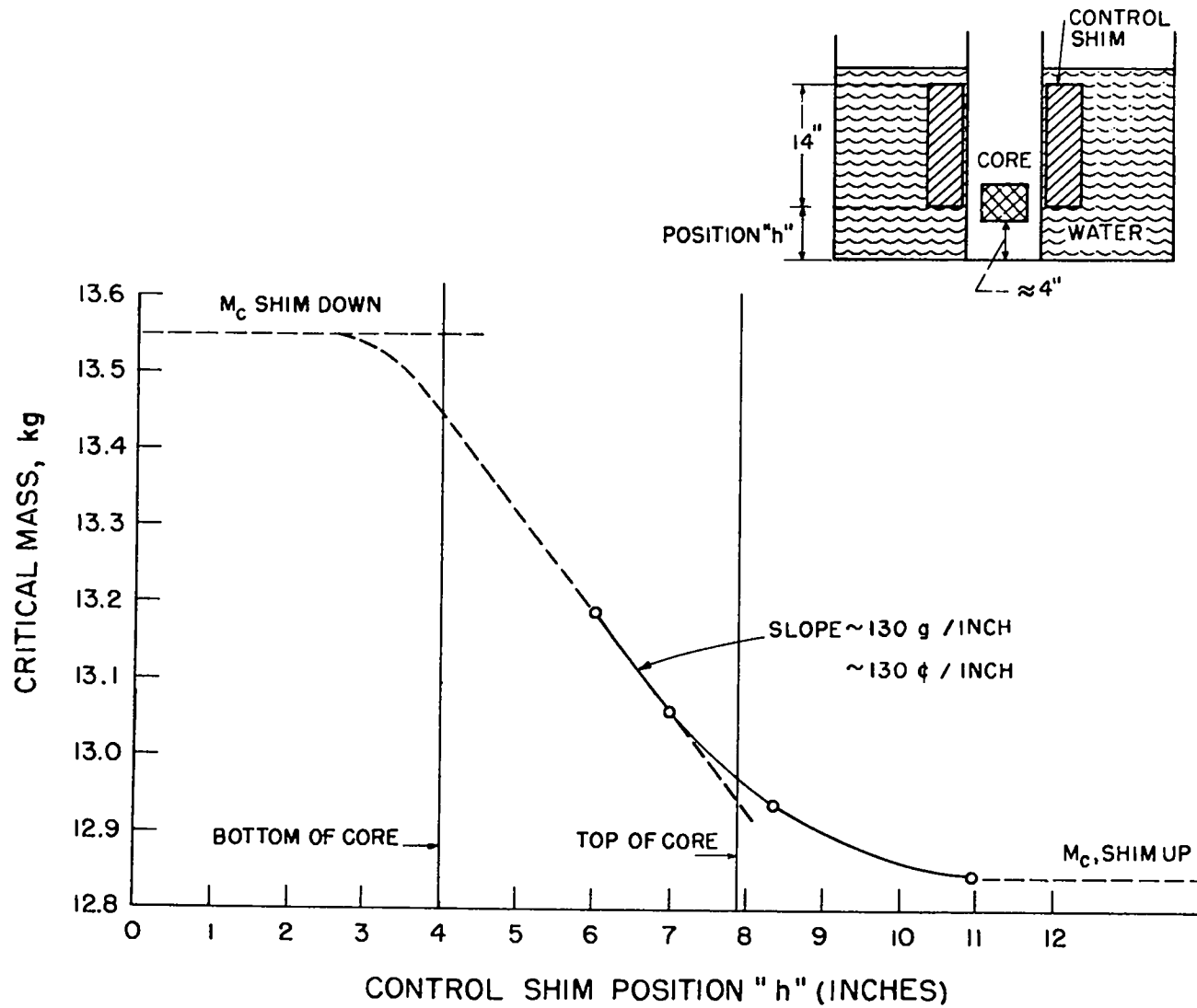
17

Fig. 2.1 L.C.X. control shim (void shim) effectiveness vs position.

critical mass. A similar result has been obtained for the LASL bare plutonium assembly Jezebel.[2] As the plutonium-tantalum core had a critical mass of 12.84 kg, 1 g of surface mass was equivalent to one cent of reactivity.

3. FISSION RATE MEASUREMENTS

A series of experiments was carried out to determine the spatial distribution of the fissions in the L.C.X. (Pu, Ta, Al) core and the integrated flux distribution in the reflector system.

Foils of U^{235} and U^{238} were irradiated at various positions in the core and in the surrounding water (Fig. 3.1). As the fission cross section of U^{235} approximates that of the Pu^{239} fuel, the power distribution in the L.C.X. core may be interpreted in terms of the U^{235} fission distribution. The activation of the U^{238} gave a gross measurement of the neutron flux over 1.2 Mev.

Thin foils of U^{235} and U^{238} (0.25 in. in diameter by 0.005 in. thick) were loaded onto a thin aluminum spacer plate in a spiral pattern (Fig. 3.2) for core irradiations. Irradiations in the water were conducted by supporting sealed foils of fissionable material on an aluminum fixture. For monitoring purposes, an additional foil was placed in a central hole in the top coolant plenum mock-up. Fission rate at the outer radius of the core was determined with a supplemental foil placed on the surface of the tantalum core cage.

The foil gamma activity, corrected for beta contribution and isotopic concentration, was measured as a function of time and compared with a master decay curve for fission product activity at a decay time $\tau = 2$ hr, to obtain relative foil fission rates. The (n,γ) reaction in U^{238} leads to significant activity when these foils are activated in thermalized fluxes, i.e., in the shield water. A correction for the U^{239} decay activity was subtracted from the measured activity by use of decay curves obtained from core foil data where the U^{239} activity, following irradiation, is small. Additional corrections due to the small
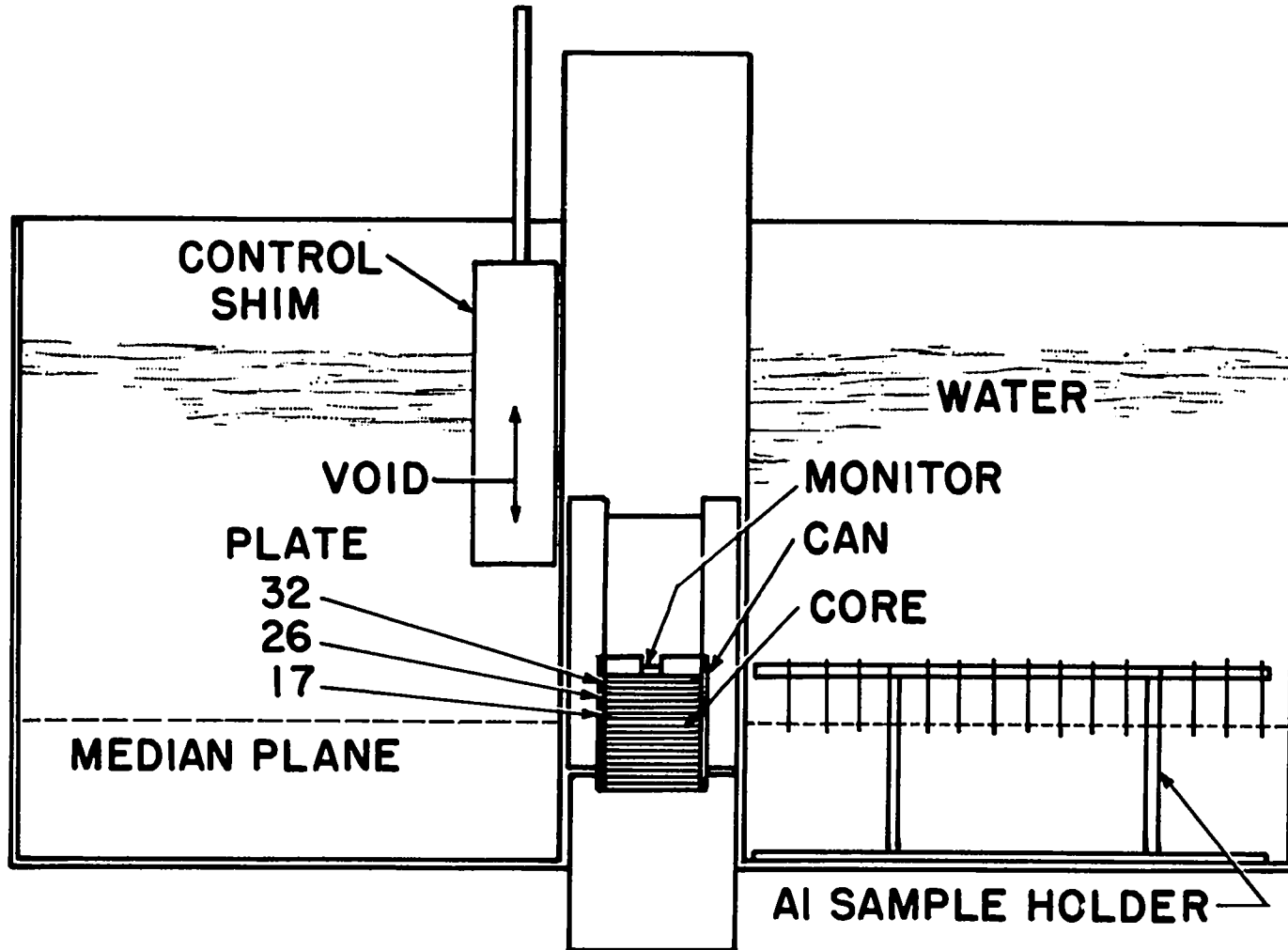
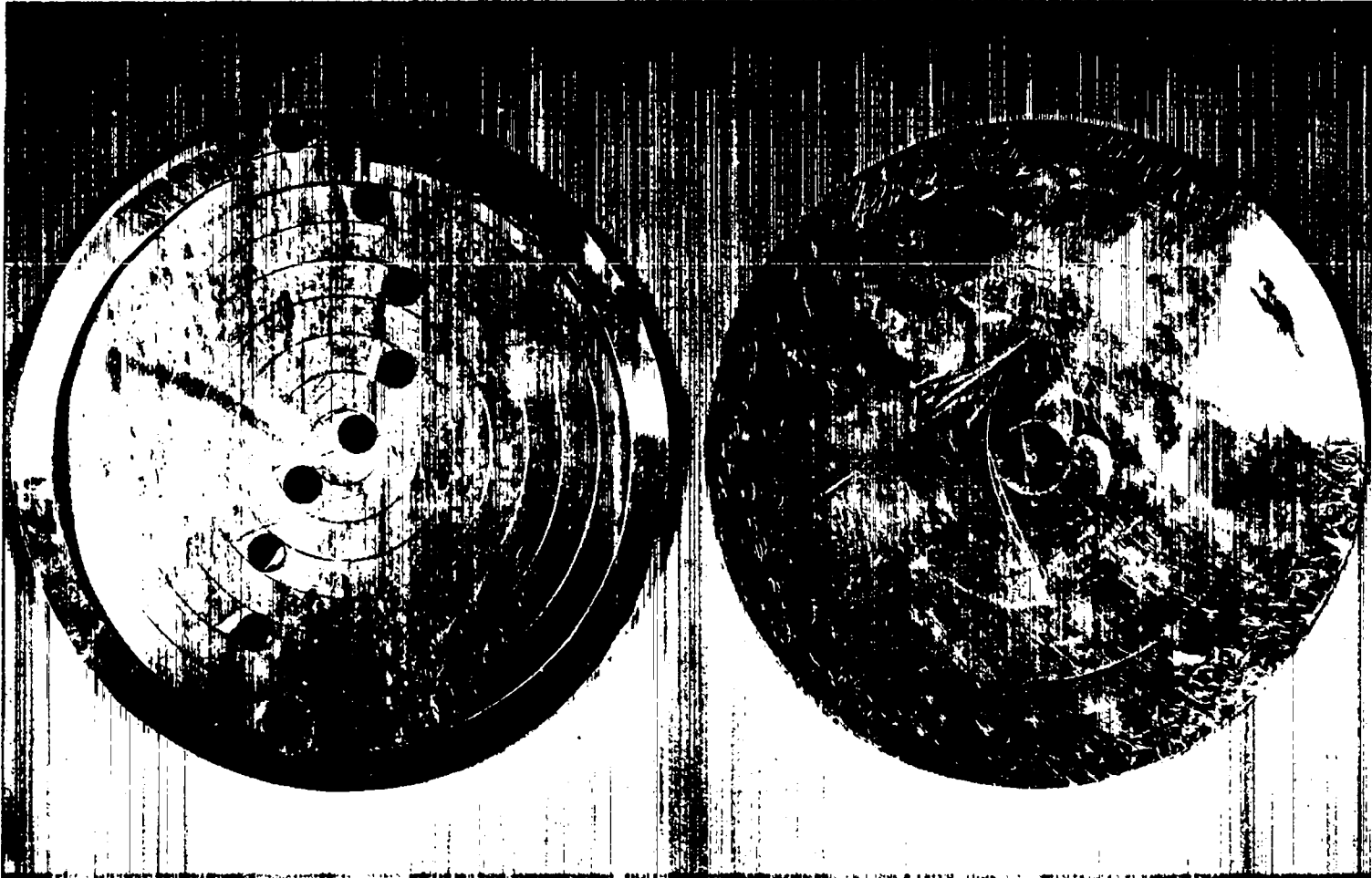Fig. 3.1 Place of foils for flux mapping in L.C.X.

Fig. 3.2 Aluminum holder for irradiation of foils in L.C.X. core.

amount of U^{235} remaining in the depleted U^{238} foils were also applied to the data. The data have not been corrected for finite foil size or for possible flux perturbations due to control shim positioning.

Median plane measurements of U^{235} and U^{238} fission rates are given in Fig. 3.3. Radial U^{235} core traverses at a few axial positions in the core are given in Fig. 3.4 and represent approximate core power distributions.

4. S_4 INTERPRETATIONS

The L.C.X. system was analyzed by a ten-group S_4 method.[3] Spherical computations were used to obtain material bucklings, reflector savings, and shim worths for the various core and reflector composites.

The critical mass of the cylinder was estimated by utilizing the computed material buckling and reflector savings in a simple cylindrical buckling formula obtained from diffusion theory.

Shim worths were analyzed in terms of an equivalent reduction in radial reflector savings. The core height was adjusted to bring the system back to critical. Hence, the shim worths are expressed as per cent increments of top surface mass to correspond to the experimental techniques used.

Reaction rates were determined by performing energy integrations pointwise over the computed fluxes.

A comparison of the computed and experimental results for critical masses and shim worths appears in Table 4.1. The trend of negative mass errors is attributed to the difficulty of including the anisotropic scattering of hydrogen into the S_4 scheme. The effective transport cross sections used for hydrogen in the S_4 scheme seem to be slightly too large. Those systems for which the neutron reflection from water is less important yield better agreement between theory and experiment (Cases 0, V, and IX).
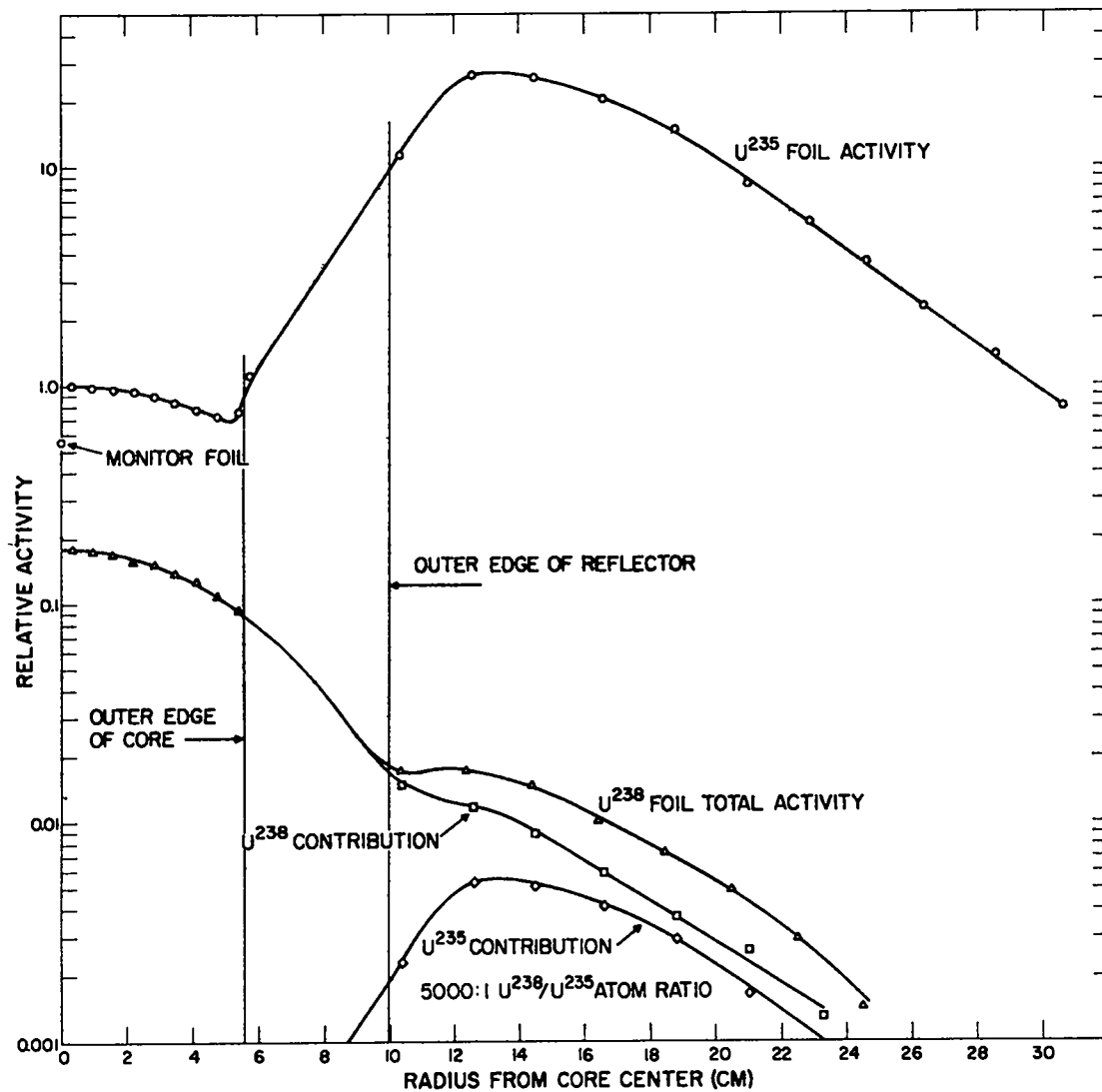
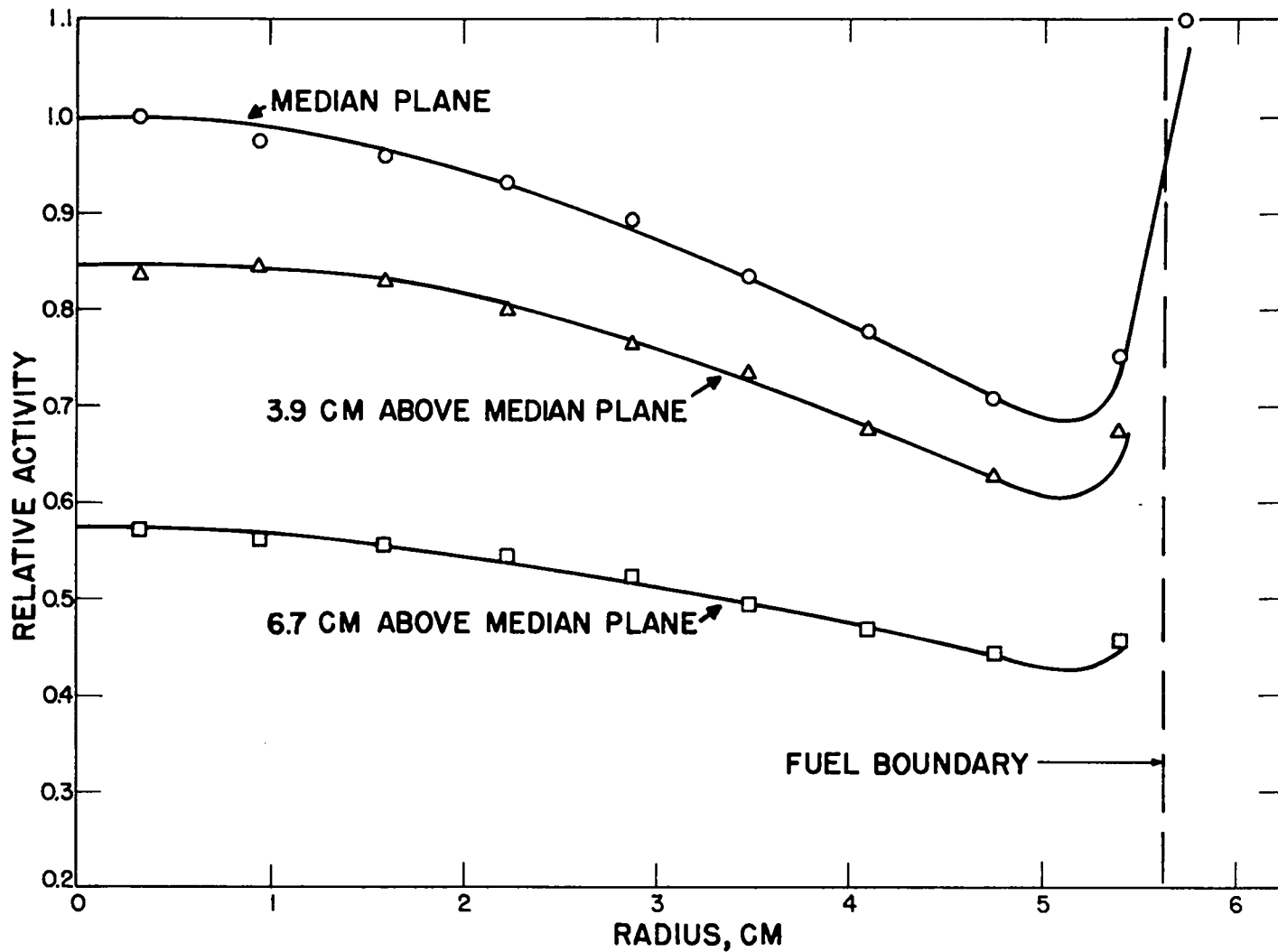Fig. 3.3 Activity of U²³⁵ and U²³⁸ foils irradiated in median plane of the L.C.X.

Fig. 3.4   Power distribution (U^{235} activation) as a function of radial and axial position in in L.C.X. core.

TABLE 4.1 COMPARISON OF COMPUTED AND EXPERIMENTAL VALUES OF CRITICAL MASSES

AND SHIM WORTHS FOR THE L.C.X. ASSEMBLIES

Case[a]	Core	Shim	S_4 M_c (kg)	Experimental M_c (kg)	ΔM/M Error (%)	S_4 Shim Worth[b] (%)	Experimental Shim Worth[b] (%)
0	Pu	Void	13.75	(13.79)[c]	-0.6	+13.8	+7.5
II	Pu, Ta	4 in. H_2O	11.57	11.87	-2.5	--	--
V	Pu, Ta	4 in. H_2O	12.08	12.84	-6.3	--	--
V	Pu, Ta	4 in. Air	13.13	13.55	-3.2	+8.7	+5.5
IX	Pu, Ta	4 in. Al	11.58	12.01	-3.5	-4.1	-6.5
X	Pu, Ta	3 in. Al	11.83	12.66	-2.5	-2.1	-1.3
XI	Pu, Ta, Al	4 in. H_2O	15.12	16.96	-10.8	--	--
XI	Pu, Ta, Al	4 in. Air	16.72	(18.16)[c]	-8.0	+10.5	+7.2

a. Except for Case 0, case numbers correspond to those in Table 2.3.

b. Shim worths are expressed as ΔM/M per cent of top surface fuel mass increments.

c. Estimated mass value.

If the overemphasis of hydrogen transport is taken into account, the computed values of shim worth agree in sign and magnitude with the experimental determinations.

Figure 4.1 shows the computed relative fission rates of U^{235} and U^{238} throughout the core and reflector for a spherical version of Case XI. These results should be compared with the experimental values given in Fig. 3.3. Both the shape and the magnitude of the fission rates are in agreement after sphere-to-cylinder corrections are made. A comparison of the computed and measured values of the relative fission rates in U^{235} and U^{238} is shown in Table 4.2.

TABLE 4.2 COMPUTED AND MEASURED VALUES OF THE RELATIVE
FISSION RATES IN U^{235} AND U^{238}

$\sigma_f(235)/\sigma_f(238)$	S_4 (Sphere)	Experimental (Cylinder)
At core center	5.7	5.6
At H_2O reflector boundary	635	770
At thermal flux peak	3200	2800

Computed flux plots for the Case V, Table 4.1, configuration are given in Figs. 4.2 and 4.3 to show the effect of the void shim control mechanism on the spatial neutron energy distribution.

REFERENCES

1. G. R. Keepin in Progress in Nuclear Energy, Vol. 1, Series 1, p. 191, Pergamon Press, London, 1956.

2. H. C. Paxton, Nucleonics 13, No. 10, 49 (1955).

3. R. M. Kiehn, "Some Applications of the S_n Method", American Nuclear Society Meeting, June, 1957.
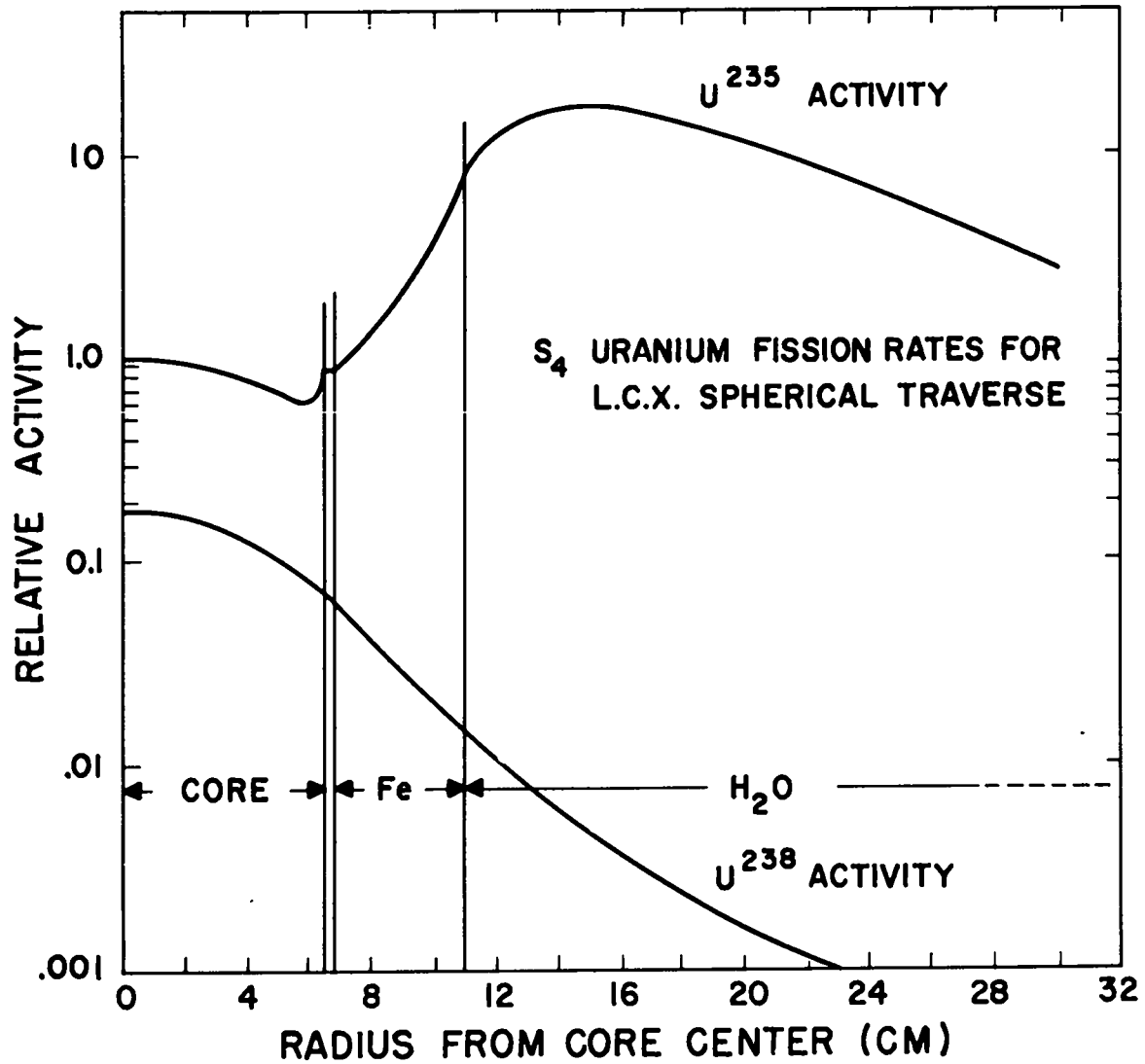
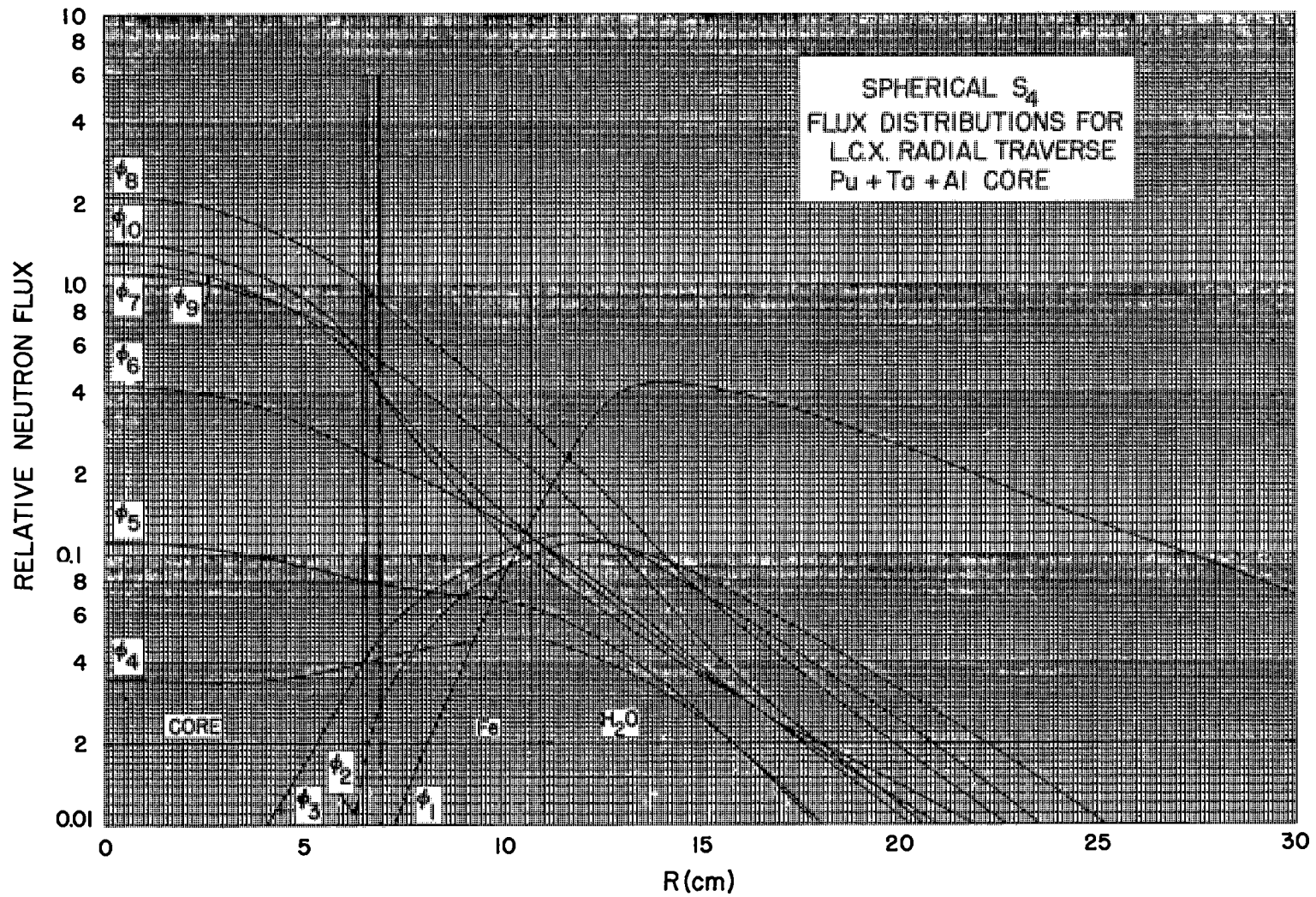Fig. 4.1   Computed radial variation of U^{235} and U^{238} activation in a spherical L.C.X. core.

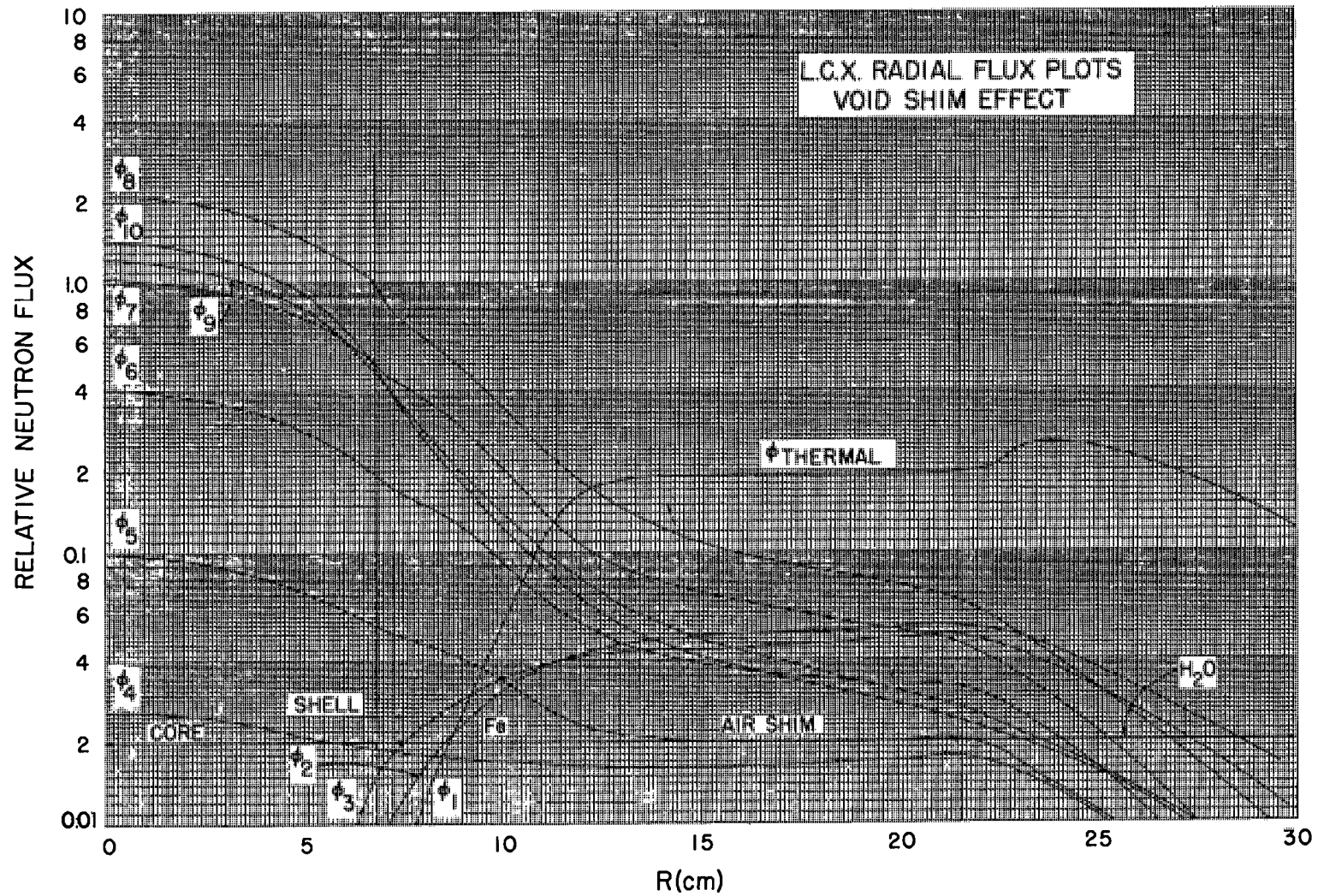Fig. 4.2 Computed radial variation of neutron flux (ten energy groups) in L.C.X.

Fig. 4.3 Calculated effect of air-filled (void) shim on the flux distribution in L.C.X.